Journal of Applied Fluid Mechanics, Vol. 13, No. 2, pp. 429-441, 2020.
Available online at www.jafmonline.net, ISSN 1735-3572, EISSN 1735-3645.
DOI: 10.29252/jafm.13.02.30146

Pressure-Driven Electro-Osmotic Flow and Mass Transport in Constricted Mixing Micro-Channels

C. Ahamed Saleel†, A. Algahtani, I. Anjum Badruddin, T. M. Yunus Khan, S. Kamangar, and M. A. H. Abdelmohimen

Department of Mechanical Engineering, College of Engineering, King Khalid University, PO Box 394, Abha 61421, Kingdom of Saudi Arabia

†*Corresponding Author Email: ahamedsaleel@gmail.com*

(Received February 9, 2019; accepted July 10, 2019)

ABSTRACT

Both micro electro mechanical systems (MEMS) based and lab-on-a chip (LoC) devices demand efficient micro-scale mixing mechanisms for its effective control which necessitates the quality research towards more efficient designs. A new venture is investigated in those direction with mixing micro-channel constricted with rectangular block under pressure-driven electro-osmotic flow and is numerically simulated by a modified immersed boundary method (IBM), an alternative technique in computational fluid dynamics (CFD). The electro-osmotic flow elucidated by electrical double layer theory when simultaneously considered with pressure driven flow in micro channels can be effectively figured out by the solution of Navier-Stokes equations linked with Nernst-Planck and Poisson equations for transportation of ion and electric field respectively. In this study, the effect of varying the height of rectangular block on the flow and mixing performance are analyzed. A hybrid method, which is a combination of active and passive techniques, is introduced simultaneously in the micro-channel by the electro-osmotic effects and channel constriction. The approach is on the basis of finite volume methodology on a staggered mesh. The governing equations are solved by a time-integration technique based on a fractional step method. The velocity fields are corrected by a pseudo-pressure term to ensure the continuity in each computational time step. The extent of mixing in every cross section of the micro channel is assessed by a suitable mixing efficiency parameter. This study has shed light on the most predominant factors that influence mixing efficiency in a micro-channel, such as geometry of the block, non-dimensional numbers (Reynolds number, *Re* and Peclet number, *Pe*), zeta potential, external electric field strength and electrical double layer (EDL) thickness. The maximum efficiency in this micro mixer design is found to be 51.3% for Reynolds number of 0.05 and Peclet number of 450 with the rectangular block height of 0.75. It is clear that both electro osmotic effects and flow perturbations due to channel constriction caused a remarkable improvement in mixing efficiency. The outcomes of this investigation are widely applicable in cooling of microchips, heat sinks of MEMS based devices, drug delivery applications and Deoxyribonucleic acid (DNA) hybridization. The present IBM model is validated by experimental and numerical results from the literature.

Keywords: Immersed boundary method; Micro-channel; Electro-osmotic flow; Electrical double layer; Mixing; Mixing efficiency; Zeta potential, MEMS.

NOMENCLATURE

C	liquid concentration
D_i	diffusion coefficient
C_p	molar concentration of cations
C_m	molar concentration of anions
C_0	bulk flow ion concentration
E_i	externally applied electric field strength
E_x	electric field in stream wise direction
e	charge of electron
f_c	concentration forcing function
f_i's	momentum forcing functions
f_x	momentum forcing function in stream wise direction
f_y	momentum forcing function in cross stream wise direction
H	channel height
k_b	boltzmann constant
L	channel length
p	pressure
Pe	Peclet number
q	mass source/sink term
Re	Reynolds number
T	temperature
t	time
u_i 's	velocity vectors
$\hat{u}$	intermediate velocity

x_i's cartesian coordinates
z valence

Subscripts

i grids in stream wise direction
j grids in transverse direction
x stream wise component
y transverse component

Superscripts

k fractional step's index
n time step
$*$ non-dimensional form

Greek Symbols

α ionic energy parameter
β *non-dimensional parameter combining* α, ω *and*
ε *dielectric constant*
ε_0 *permittivity of the fluid*
Δt *computational time step*
μ dynamic viscosity
λ Debye length or EDL thickness
ρ fluid density
ρ_e electric charge density
ϕ pseudo-pressure
ψ electro-osmotic potential
ζ zeta potential (varied in steps of -25mV)
ω Debye-Huckel parameter
σ mixing efficiency

Abbreviations

CFD Computational Fluid Dynamics
DNA Deoxyribonucleic acid
EOF Electro-Osmotic Flow
EDL Electrical Double Layer
FVM Finite Volume Method
IBM Immersed Boundary Method
LES Large Eddy Simulation
MEMS Micro-Electro Mechanical Systems
RK3 Third order Runge Kutta
ADI Alternating Direction Implicit
TDMA Tri-Diagonal Matrix Algorithm

1. INTRODUCTION

Liquid flow and mixing in micro-channels have extensive applications in industry, such as cooling of microchips, heat sinks of MEMS based devices, estrangement of biological components within microfluidic chips used in drug delivery applications, DNA hybridization, and so on (Yang *et al*., 2001; Babaie *et al*., 2011; Cho, 2007; Bayraktar and Pidugu, 2006; Mollajan *et al*., 2018; Banerjee *et al*., 2019). In addition to the use of electro-osmotic effects in pressure-driven flow, restriction in micro-channels by means of rectangular blocks of varied height is an innovative idea to enhance the mixing efficiency. The general sketch of the present problem is shown in Fig. 1.

It not only incorporates active and passive mixing techniques (hybrid technique), but also allows simpler fabrication and a consistent operation and control. As the constriction in micro-channels is made with rectangular blocks of varied height, numerical simulation with a modified IBM considerably reduces the computational cost and time by considering the blocks as an immersed boundary (IB).

Despite several significant developments in CFD, some elementary problems such as accuracy, efficiency of computation and capacity to handle complicated geometries remain an ongoing challenge (Kim *et al*., 2001; Saleel *et al*., 2011). These problems could be tackled by IBM, wherein the presence of a complex boundary is replaced by a time-spatially varying distribution of a forcing term. Even though significant progress has been reported by various researchers in complex flows (Baum *et al*., 1998; Ramamurti and Sandberg, 2001; Tezduyar, 2001; Saleel *et al*., 2013), the IBM qualifies as an attractive alternate option. The illustrious simplicity of IBM is utilization of the Cartesian grids for the whole simulations. The use of IBM dates back to 1972 (Peskin, 1972) for the simulation of cardiac mechanics and associated flow of blood. A forcing function/term accompanied by the Navier-Stokes equations is responsible for fluid-solid interactions. A detailed survey on IBM was provided by Mittal and Iaccarino (2005), and its application was reported in various fluid dynamics problems (Wang *et al*., 2009; Ren *et al*., 2013; Azis *et al*., 2019).

The discovery of electro-kinetic transport (Reuss, 1809) paved the way for detailed study of liquid flows in capillary porous systems affected by external electric fields. Theoretical studies in this area include simulation of joint pressure driven-electro-osmotic flows in two-dimensional micro-channels (Burgreen and Nakache, 1964; Ohshima and Kondo, 1990; Dutta and Beskok, 2001) and thin cylindrical capillaries (Rice and Whitehead, 1965; Lo and Chan, 1994; Keh and Liu, 1995; Santiago, 2001). Review of the current experimental works in this area is available in (Molho *et al*., 1998; Paul *et al*., 1998; Cummings *et al*., 1999; Kim *et al*., 2002; Herr *et al*., 2000). Electro-osmosis and electrophoresis are the two routinely used electro-kinetic effects in micro and nano-scale transport applications. The electro-osmosis phenomenon stems from the electric double layer (EDL) theory postulated by Helmholtz (Probstein, 2005), and detailed insights into this theory are well documented by Jens *et al*. (2010). Debye layers formed due to the accrual of static charges on the walls of a micro-channels due to its dielectric nature and subsequently initiated electro-osmotic flow with proper electric field are well explained in Jens *et al*. (2010).

Numerical investigations of electro-osmotic transportation have been widely reported. For instance, Yang and Li (1998) developed a numerical algorithm based on Debye-Huckel approximation, and analysed electro-kinetic phenomena in

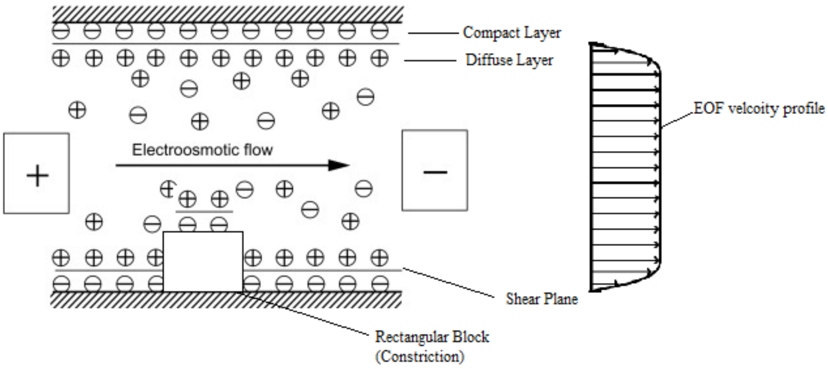

Fig. 1. Electro osmotic effects in micro-channel with constriction.

pressure-driven liquid flows. An algorithm based on FVM to study micro-fluidic injection by means of electro-osmotic forces through intersection of two channels was proposed by Patankar and Hu (1998). They found that, substantial inertial effects were present for the flows with Reynolds number (*Re*) > 1, which was in agreement with the findings of Santiago (2001). A finite element formulation was used by Bianchi *et al.* (2000) to model flow in a T-channel junction with electro-osmotic effects. A spectral element algorithm was established by Dutta *et al.* (2002a, 2002b) for the solution of pressure-driven electro-osmotic flows in complex geometries. Bera and Bhattacharyya (2013) performed a detailed numerical simulation to analyze similar kind of flows with species transport in micro/nano-channels and studied the effects of *Re* for both thin and overlapped cases of EDL. Ebrahimi *et al.* (2014) studied mixing and heat transfer characteristics of pressure driven-electro-osmotic flow in a T-shaped micro-channel by carrying out a numerical simulation and predicted some means to improve efficiency of mixing in micro-channel. Bhattacharyya and Bera (2015) numerically investigated pressure-driven electro-osmotic flow in an infinitely long micro-channel with surface roughness.

1.1. Recent Theoretical and Field Studies

Qaderi *et al.* (2019) carried out numerical simulation of combined pressure driven electro osmotic mixing in a micro-channel incorporated with triangular hurdle and zeta-potential heterogeneity. They identified that mixing efficiency is boosted due to increase in pressure gradient, zeta potential heterogeneity and hurdle height. Banerjee *et al.* (2019) found out that geometric parameter of wavy side walls of the micro channels influence the mixing efficiency along with solution's molarity and electric field strength.

The diffusion time is the ratio of the square of channel characteristic length to the mass diffusion coefficient as $\tau_d = \frac{L^2}{D}$. Generally, the mass diffusivity of liquid, *D* is quite small, especially for large molecules like DNA and proteins, whose diffusion coefficients are in the order of 10^{-2}m/s^2 or less. In micro-channels, inertia forces are amazingly feeble and hence turbulence does not occur. Without turbulence, it is hard to enhance the mixing simply by diffusion, and hence the subsequent mixing time and mixing length can be exceptionally long and unrealistic. This warrants the need of an effective micro-mixer that provides quick mixing for many applications such as DNA hybridization, cytometric analysis and immuno analysis. Many researchers have proposed variety of mixers to augment the mixing effectiveness.

1.2. Significance and Novelty

A modified IBM, an alternative technique in CFD, has been used to investigate the pressure driven electro-osmotic flow and mixing in a constricted micro-channel. Since electro-osmotic effects and channel constriction simultaneously incorporate the active and passive mixing techniques in micro-channel, it may be considered as a hybrid technique to enhance the mixing efficiency in micro-channel. Constrictions in micro-channel (rectangular block) can be easily and effectively simulated numerically by using IBM, as the height of the rectangular block is varied, compared to conventional CFD approaches. Concentration forcing function (first time in the literature) is defined to satisfy and imitate the no-flux boundary condition for species concentration on the block (immersed boundary) and is introduced in convection-diffusion equation.

The previous studies have considered a constant height of the rectangular block, and the effect of varying the block-height has not been reported, which is the focus of the current study. Conventional CFD techniques are used for the numerical simulations in all previous works, whereas a modified IBM is employed in the present work. This hybrid technique eliminates almost all disadvantages pertaining to general active and passive mixing methods in micro channels (Ahmed *et al.*, 2009; Luong *et al.*, 2011; Campisi *et al.*, 2009; Mahammedi *et al.*, 2017; Islami *et al.*, 2017; Ababaei *et al.*, 2017; Cho, 2008; Lim *et al.*, 2010; Du *et al.*, 2010; Buchegger *et al.*, 2011; Neerincx *et al.*, 2011; Isfahani *et al.*, 2018; Nayak *et al.*, 2018; Borgohain *et al.*, 2018; Chen *et al.*, 2019; Fan *et al.*, 2019).

First, mathematical modelling is presented which includes computational domain, required governing equations with suitable boundary conditions and solution methodology. Then, results and discussion

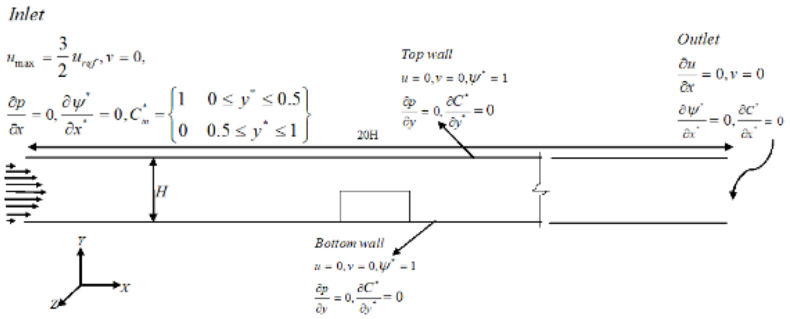

Fig. 2. Computational domain with boundary conditions for pressure-driven electro-osmotic flow and mixing in a micro-channel constricted with a rectangular block.

elaborate grid dependency, model validation and significant results with due explanations. A parameter for mixing efficiency was appropriately adopted from the literature to compute the effectiveness of mixing in every cross-section of the micro-channel. The article is concluded with the major achievements, advantages, disadvantages and limitations of the study.

2. MATHEMATICAL MODELLING

To compare and select a suitable IBM to be modified and extended for the present problem, all the IBMs developed so far were analyzed by considering the following factors: (i) easiness in implementation, (ii) conservation of mass, (iii) appropriateness with high Re, (iv) turbulence/large eddy simulation (LES), (v) suitability with staggered grid, (vi) aptness with 3D problems, (viii) suitability with moving boundaries, (ix) severity in restriction of time step, (x) second-order accuracy in space and (xi) discretization of convection and diffusion terms (explicit or implicit). As suitability with high Re is not significant for the present problem, the mass source/sink approach proposed by Kim *et al.* (2001) was found to be appropriate after analyzing the pros and the cons of the rest of the techniques. The mass source term as well as a momentum forcing functions for flows over or inside intricate geometries were incorporated in the model.

2.1 The Computational Domain

The computational domain for the flow through micro-channel restricted with rectangular blocks is shown in Fig. 2. The blocks in the micro-channel are taken care of by corresponding forcing functions in the momentum and species conservation equations. Specific boundary conditions need not be specified for the block, which is the major advantage of IBM. The flow was assumed as unsteady in the whole computational domain. The buoyant forces were assumed to be negligible with respect to viscous and pressure forces.

For species concentration the boundary condition is stated at the inlet as follows:

$$C_{in}^{*} = \begin{cases} 1 & 0 \le y^{*} \le 0.5 \\ 0 & 0.5 \le y^{*} \le 1 \end{cases}$$

i.e., Stream A enters the mixing channel with a concentration of $C_{in}^{*} = 0$ *via* the upper inlet, while stream B enters from the lower inlet with a concentration of $C_{in}^{*} = 1$.

2.2 Governing Equations and Solution Methodology

The unsteady incompressible pressure-driven electro-osmotic viscous fluid flow and mixing is governed by the Navier-Stokes (momentum), continuity and convection-diffusion equations, as presented below:

$$\frac{\partial u_i}{\partial t} + \frac{\partial (u_i u_j)}{\partial x_j} = -\frac{1}{\rho}\frac{\partial p}{\partial x_i} + \frac{\mu}{\rho}\frac{\partial^2 u_i}{\partial x_j \partial x_j} + \frac{\rho_e}{\rho} E_i + f_i \quad (1)$$

$$\frac{\partial u_i}{\partial x_i} - q = 0 \quad (2)$$

$$\frac{\partial C}{\partial t} + \frac{\partial (u_i C)}{\partial x_j} = D_i \frac{\partial^2 C}{\partial x_j \partial x_j} + f_c \quad (3)$$

The forcing function 'f_c' in Eq. (3) is the contribution of the present model, which is introduced to mimic the constrictions. The dissemination of ions in the buffer solution is influenced by the static charge on the surface, which is determined by the Poisson-Boltzmann equation given in Appendix as Eq. (I).

The assumptions made in the present simulation are:

- ✓ The local electric field strength does not affect the fluid viscosity.
- ✓ Ions are in stability with the electric charge on the wall, which justifies the use of Poisson-Boltzmann equation for the dissemination of electro-osmotic potential.
- ✓ The fluids are continuous and fully satisfy the continuum assumption.
- ✓ The overall and local electric field strengths do not influence the permittivity of fluids.
- ✓ The ions are point charges.
- ✓ Electric conductivity is constant and Joule heating effect is negligible.
- ✓ The fluid viscosity is free of the shear rate. Hence, fluids are assumed to be Newtonian.

- ✓ The thermo-physical properties of the fluids are constant.
- ✓ The flow is incompressible and two dimensional.
- ✓ Buoyant forces are negligible compared with viscous and pressure forces.
- ✓ External electric field is applied only in the stream-wise direction.

Modification and normalization of governing equations are explained in Appendix. The appropriately modified non-dimensional momentum, continuity and species transport equations are

$$\frac{\partial u_i^*}{\partial t^*}+\frac{\partial(u_i^* u_j^*)}{\partial x_j^*}=-\frac{\partial p^*}{\partial x_i^*}+\frac{1}{Re}\frac{\partial^2 u_i^*}{\partial x_j^*\partial x_j^*}+\frac{1}{Re}\beta\sinh\left[\alpha\psi^*\right]+f_i^* \tag{4}$$

$$\frac{\partial u_i^*}{\partial x_i^*}-q^*=0 \tag{5}$$

$$\frac{\partial C^*}{\partial t^*}+\frac{\partial(u_i^* C^*)}{\partial x_j^*}=\frac{1}{Pe}\frac{\partial^2 C^*}{\partial x_j^*\partial x_j^*}+f_C^* \tag{6}$$

The basis of temporal discretization method used to solve the flow field and species transport equations (4) to (6) is fractional step method. The third-order Runge–Kutta method (RK3) and second-order Crank–Nicolson method are used for the convection and diffusion terms respectively. In the flow equations, the continuity equation is verified in every time step by correcting the velocity field with the help of a pseudo-pressure. The overall solution methodology involves solving of Eq. (VI) in appendix followed by Eq. (4) through (6) subjected to the boundary conditions shown in Fig. 2. The momentum forcing function, mass source term and concentration forcing function need to be calculated to represent immersed boundaries present, if any. Staggered Grid is utilized where in the pressure is defined at the cell centers and velocities are defined normal to the cell faces (Harlow and Welch, 1965).

3. RESULTS AND DISCUSSION

3.1 Grid Dependency

It is ensured that the grid generated has sufficient accuracy in predicting the physics involved. The grid independence test is done with respect to mixing in a straight micro-channel of height, H=60 μm and length, L=1200 μm. The simulation is run for four different grid resolutions, namely, 127×27, 252×52, 502×102 and 1002×202. The concentration profile at the channel outlet is plotted for all the four cases in Fig. 3 which justifies choosing a grid size of 502×102.

3.2 Model Validation

The present computational model is validated with the published works in the literature. The electro-osmotic flow velocity profile predicted by present model is compared with the experimental results of Dutta *et al*. (2001), while the mixing efficiency is compared with the findings of Wang *et al*. (2007), for similar dimensions and operating conditions. It is obvious from Figs. 4(a) and (b) that the present predictions are in excellent agreement with the experimental results. For further verification of mixing efficiency in a micro-channel constricted with rectangular block, a comparison was made with the model presented by Chang and Yang (2004) and found to be in reasonable agreement, as depicted in Fig. 4(c).

In order to measure the extent of mixing in every cross section of the mixing micro-channel, a mixing efficiency parameter (σ) is adopted from Aubin *et al.* (2005).

$$\sigma(x)=\left(1-\frac{\int_0^H\left|C-C_\infty\right|dy}{\int_0^H\left|C_0-C_\infty\right|dy}\right)\times 100\% \tag{7}$$

where C is the species concentration profile across the width of the mixing channel, and C_0 and C_∞ are the species concentrations with completely unmixed (0 or 1) and completely mixed states (0.5), respectively.

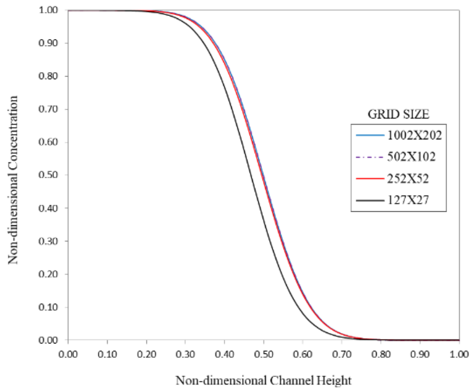

Fig. 3. Grid Independency: Concentration profile at the channel outlet in a straight mixing channel.

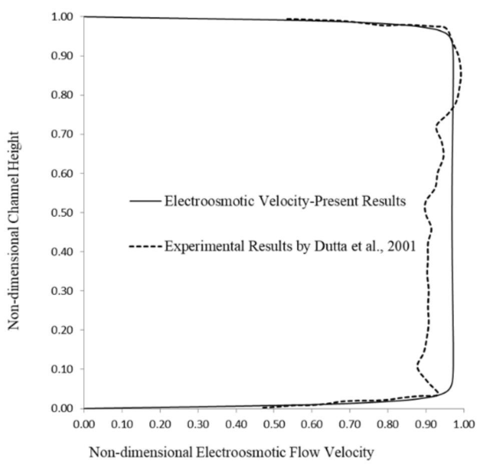

Fig. 4. (a) Validation with Dutta *et al.* (2001).

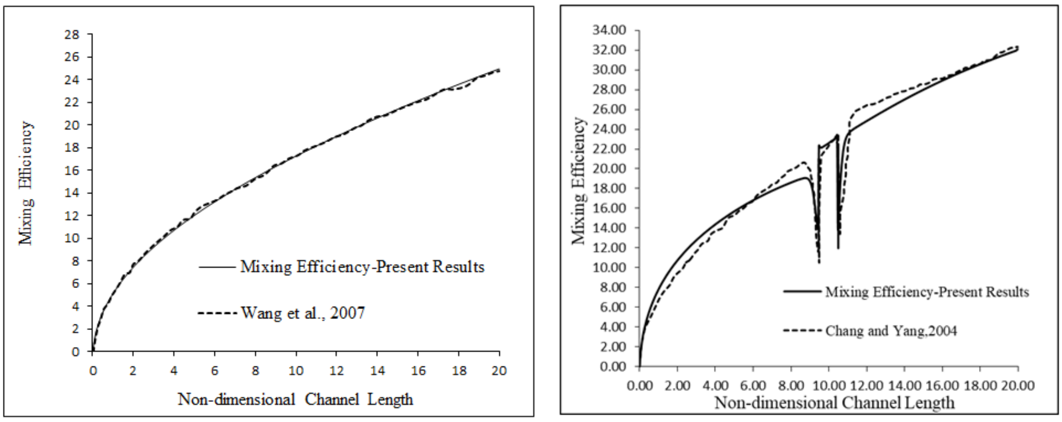

Fig. 4. (b) Validation with Wang *et al.* (2007) and (c) Validation with Chang and Yang (2004).

3.3 Pressure Driven Electro-Osmotic Flow and Mixing in Constricted Micro-Channel

In order to speed up the mixing process in micro-fluidic systems, a rectangular block of varied height is incorporated in the micro-channel that actually causes transverse flow across the channels. Effect of non-dimensional numbers (Re and Pe), zeta potential, external electric field strength and electrical double layer (EDL) thickness on mixing efficiency is studied by varying the height of the incorporated rectangular block. The values of physical parameters for the present simulation is adopted from [63-65] and is shown in nomenclature section. Turbulent flow is almost impossible to achieve in micro-fluidic systems. The reason for the same is extremely low Reynolds numbers prevalent in the micro-channel flow. Exciting flow in the lateral direction across the micro-channel is an excellent approach to cause additional mixing, since it should enhance the diffusive mixing process. The variation in transverse flow velocity is possible by changing the height of the rectangular block. Figures 5(a) and (b) present the stream wise velocity contour and transverse velocity contour with a rectangular block of 30µm high and 120 µm wide for Re=0.2 (Pe=1800), respectively. It is vivid to visualize that the maximum stream-wise velocity is present just above the rectangular blocks.

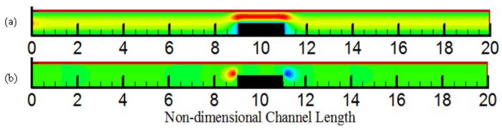

Fig. 5. Mixing channel with one rectangular block of non-dimensional height= 0.5: (a) Stream wise velocity distribution (b) Transverse velocity distribution (*Re*=0.2).

Figure 5 shows that separation of flow does not occur over the rectangular block due to electro-osmotic effects considered along with pressure driven flow. The separation of flow takes place in pure pressure-driven flow even at very low Reynolds numbers. Absence of flow separation is a quite different phenomenon specially observed in in micro-channels. The reason for the absence of flow separation is the electro osmotic flow in which the influential force responsible for instigating the same is due to interaction of the EDL with the external electric field and is given by the whole EDL in the region of the solid wall surfaces of the micro-channels. The movement of the fluid exterior to the EDL is hauled by the fluid inside the EDL. Subsequently, the electro osmotic force is able to maintain the electro osmotic flow without separation.

3.3.1. Effect of Non-Dimensional Numbers (Re and Pe)

The influence of Re and Pe are investigated on the mixing efficiency. To facilitate the same, three different reference (electro-osmotic) velocity values are assumed and the value of Re and Pe are tabulated (Table 1). For the present simulation the value of wall potential is kept constant i.e., -25 mV (α=1) there by the accuracy of the numerical model can be improved by utilizing the Debye-Hückel approximation and the EDL thickness λ = 600 nm (β=10000). The value of Ex shows an increasing trend when Re and Pe values are increased.

Table 1 The values of reference velocity and external electric field strength for different Re and Pe

u_{ref} (m/s)	E_x(V/cm)	Re	Pe
0.00075	381.25	0.05	450
0.0015	762.5	0.1	900
0.003	1525	0.2	1800

Figures 6(a)-(c) describes the distribution of species concentration in the micro mixing channel constricted with a rectangular block of non-dimensional height=0.25 when Re=0.2 (Pe=1800), Re=0.1 (Pe=900) and Re=0.05 (Pe=450) respectively. The corresponding species concentration profiles at the outlet of the micro-channel are presented in Fig. 7. Figure 8 shows the mixing efficiency in every cross section throughout the mixing channel for the respective Re and Pe. The mixing efficiency is maximum (33%) when *Re*=0.05 (*Pe*=450). The mixing efficiency is 29% when *Re*=0.1 (*Pe*=900). The mixing efficiency is least for *Re*=0.2 (*Pe*=1800) and is equal to 23%. The increased reference velocity results an increase in *Re* (and *Pe*) which leads to the decrease in mixing efficiency.

Figures 9(a), (b) and (c) describes the distribution of species concentration due to mixing in the micro-channel for the case of a rectangular block of non-dimensional height=0.5 when *Re*=0.2 (*Pe*=1800), *Re*=0.1 (*Pe*=900) and *Re*=0.05 (*Pe*=450) respectively. The respective species concentration profiles at the outlet of the micro-channel are presented in Fig. 10. Figure 11 indicates the mixing efficiency at each cross section along the micro-channel for the respective *Re* and *Pe*. The mixing efficiency is maximum (49%) when *Re*=0.05 (*Pe*=450). The mixing efficiency is 47% when *Re*=0.1 (*Pe*=900). The mixing efficiency is least (44%) for *Re*=0.2 (*Pe*=1800).

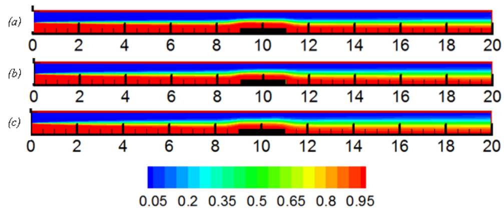

Fig. 6. Species concentration distributions for the mixing channel with a rectangular block of non-dimensional height = 0.25: (*a*) Re=0.2 (Pe=1800), (*b*) Re=0.1 (Pe=900), and (*c*)Re=0.05 (Pe=450).

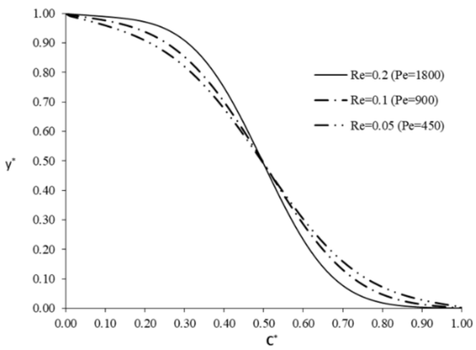

Fig. 7. Species concentration profiles at the outlet of the micro-channel constricted with a rectangular block of non-dimensional height=0.25 for different *Re* (*Pe*).

Figures 12(a), (b) and (c) describes the distribution of species concentration in the micro-channel for the case of a rectangular block of non-dimensional height=0.75 when *Re*=0.2 (*Pe*=1800), *Re*=0.1 (*Pe*=900) and *Re*=0.05 (*Pe*=450) respectively. The relevant species concentration profiles at the outlet of the micro-channel are presented in Fig. 13. Figure 14 indicates the mixing efficiency at each cross section along the micro-channel for the respective *Re* and *Pe*. The mixing efficiency is maximum (51.3%) when *Re*=0.05 (*Pe*=450). Minor changes in mixing efficiency is noticeable when *Re*=0.1 (*Pe*=900) and *Re*=0.2 (*Pe*=1800). Here also the mixing efficiency is enhanced as the *Re* and *Pe* is decreased. The magnitude of enhancement in mixing efficiency is more compared to former cases. It is to be noted that increase in *Re* results convection dominated mixing which consequently leads to a high *Pe*. Convective and diffusive flux consequently affects the mixing process. The results give an inference that with the increase of *Re* and *Pe*, an increase in micro-channel length is required to have a completely mixed state.

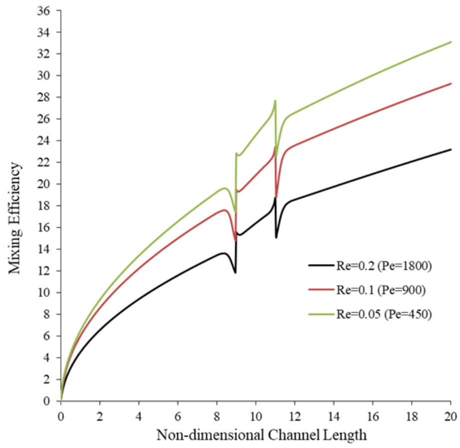

Fig. 8. Augmentation of species mixing efficiency attained by varying the Re and Pe values with a rectangular block of non-dimensional height =0.25 as an immersed boundary.

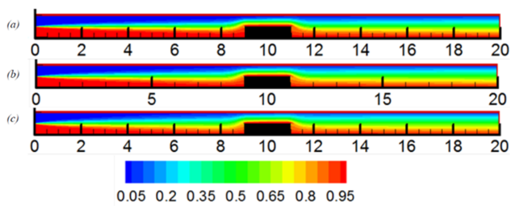

Fig. 9. Species concentration distributions due to mixing in a micro-channel constricted with a rectangular block of non-dimensional height =0.5: (*a*) *Re*=0.2 (*Pe*=1800), (*b*) *Re*=0.1 (*Pe*=900), and (*c*) *Re*=0.05 (*Pe*=450).

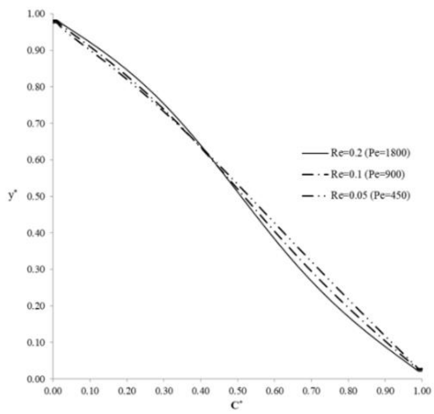

Fig. 10. Species concentration profiles at the outlet of the micro-channel constricted with a rectangular block of non-dimensional height=0.5 for different *Re* and *Pe*.

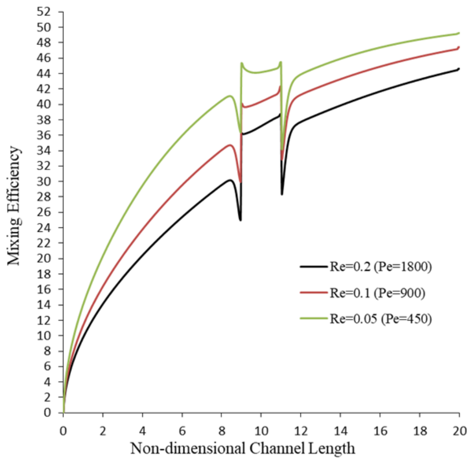

Fig. 11. Enhancement of species mixing efficiency obtained by varying the Reynolds number and Peclet number with a rectangular block of non-dimensional height =0.5 as an immersed boundary.

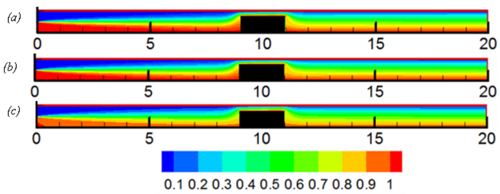

Fig. 12. Species concentration distributions for the mixing channel with a rectangular block of non-dimensional height =0.75 as an immersed boundary: (a) *Re*=0.2 (*Pe*=1800), (b) *Re*=0.1 (*Pe*=900), and (c) *Re*=0.05 (*Pe*=450).

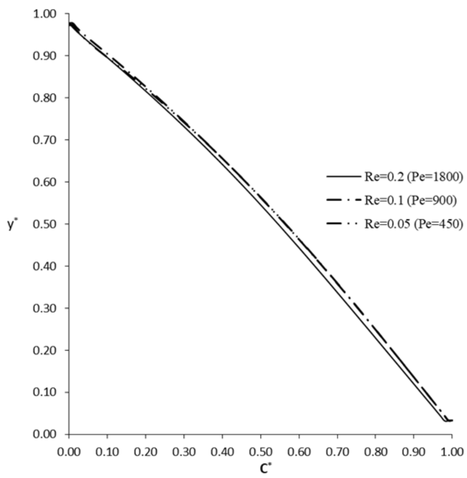

Fig. 13. Species concentration profiles at the outlet of the micro-channel constricted with a rectangular block of non-dimensional height=0.75 for different *Re* (and *Pe*).

The simulation results endorse that mixing of species is purely diffusive in nature in a straight mixing micro-channel. The insertion of rectangular blocks in the mixing micro-channel supports an improved mixing of species by compelling the bulk flow to pass through a confined micro-channel region (Figs. 6-14). It creates a stronger diffusion effect when the value of Re and Pe is decreased, thereby leads to an extra even distribution of species concentration far downstream. This results in an augmented mixing efficiency in the micro-channel. The numerical simulation results endorse that the notable augmentation of mixing efficiency in micro-channel is feasible with the introduction of rectangular blocks. But the further improvement in mixing efficiency is possible by the extension of length of the micro-channel which is not practical in majority of the microfluidic devices. The time for diffusion by lowering the flow rate can be extended by decreasing the strength of the external electric field within its specified range to drive the electro osmotic flow. It is reported that the overall percentage increase in the mixing efficiency is 10 % in a mixing micro-channel constricted with a rectangular block having non-dimensional height of 0.25 (Fig. 8) when the value of Re (and Pe) is dropped or when the value of Ex is decreased accordingly. In a mixing micro-channel constricted with a rectangular block of non-dimensional height 0.5 (Fig. 11), the overall percentage increase in the mixing efficiency is 5 % when the value of Re (and Pe) is dropped or when the value of Ex is decreased accordingly. The overall percentage increase in the mixing efficiency is 1.3 % in the case of a mixing micro-channel constricted with rectangular block of non-dimensional height 0.75 (Fig. 14) when the value of Re (and Pe) is dropped or when the value of Ex is decreased accordingly. The maximum mixing efficiency is for the case of constriction with a rectangular block of non-dimensional height of 0.75 when Re=0.05 (Pe=450) and is 51.3 %. The outcome of the study is that mixing efficiency is increasing by decreasing the Re and Pe values. It is to be noted that the Reynolds number and Peclet number are inter related. This is due to the fact that as the Re is decreased, the flow becomes highly laminar which itself is the property of electro-osmotic flow and stronger convective diffusion effects are generated in the micro-channel.

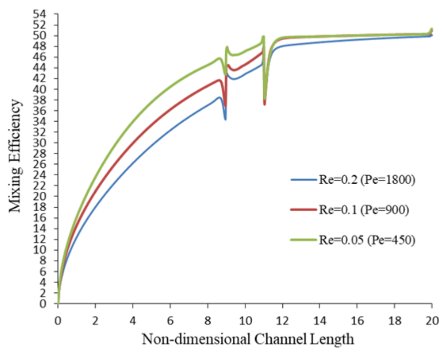

Fig. 14. Enhancement of species mixing efficiency obtained by varying the Reynolds number and Peclet number with a rectangular block of non-dimensional height =0.75 as an immersed boundary.

3.3.2. Effect of Block Height on Mixing Efficiency

To analyze the effect of the mixing efficiency on the height of rectangular blocks (constriction) in a micro-channel, numerical experimentations were carried out with block heights of 0.25, 0.5 and 0.75. Figure 15 shows the species concentration profiles due to mixing at the outlet of micro-channel at Re=0.2 (Pe=1800) for the aforesaid three different heights. Figure 16 shows the species concentration profiles due to mixing at the outlet of the micro-channel at Re=0.1 (Pe=900). Figure 17 shows the species concentration profiles due to mixing at the outlet of the micro-channel at Re=0.05 (Pe=450). It is vivid that for a particular Re (Pe), the species concentration profiles become more flat as the height of the rectangular block is increased. Figure 18 shows the enhancement of species mixing efficiency by varying the rectangular block height at Re=0.2 (Pe=1800). Figure 19 depicts the augmentation of species mixing efficiency by varying the rectangular block height at Re=0.1 (Pe=900). Figure 20 depicts the increase of species mixing efficiency by varying the rectangular block height at Re=0.05 (Pe=450). It is clear that for a particular Re (Pe), the species mixing efficiency is increased as the block height is increased. By constricting the micro-channel with the rectangular blocks of varied heights, the average velocity is increased due to reduction in area of cross section of the channel and high wall shear stress. This consequently leads to convection dominated mixing.

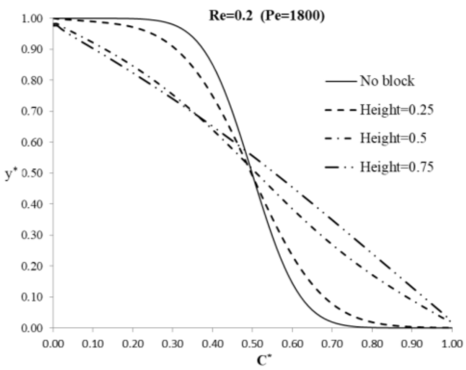

Fig. 15. Effect of block height on species concentration profiles at the outlet regions of mixing micro-channel at *Re*=0.2 (*Pe*=1800).

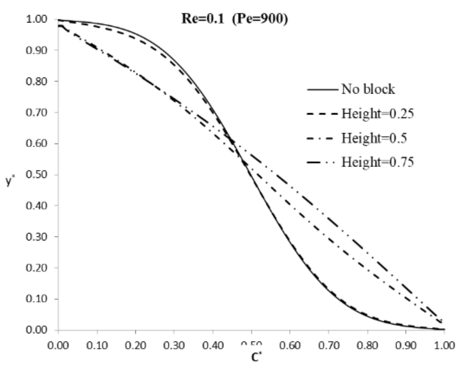

Fig. 16. Effect of block height on species concentration profiles at the outlet regions of mixing micro-channel at *Re*=0.1 (*Pe*=900).

The mixing efficiency is tabulated (Table 2) for different *Re, Pe* and rectangular block height. For a particular *Re* and *Pe*, the mixing efficiency is maximum for rectangular block of non-dimensional height 0.75 and is least for rectangular block having non-dimensional height 0.25.

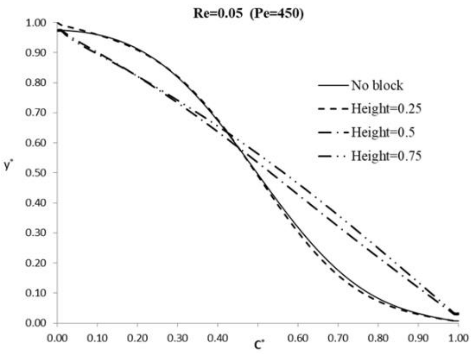

Fig. 17. Effect of block height on species concentration profiles at the outlet regions of mixing micro-channel at *Re*=0.05 (*Pe*=450).

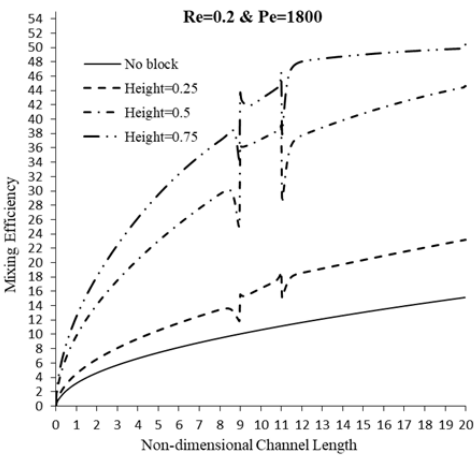

Fig. 18. Enhancement of species mixing efficiency obtained by varying the block height at *Re*=0.2 (*Pe*=1800).

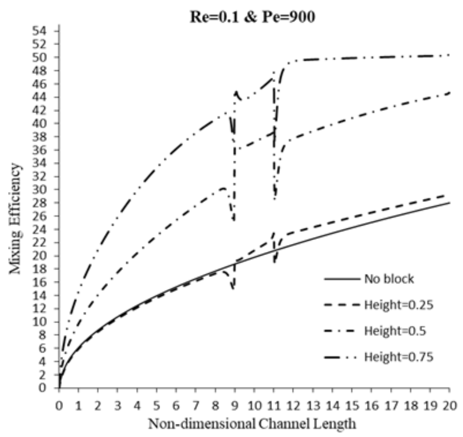

Fig. 19. Enhancement of species mixing efficiency obtained by varying the block height at *Re*=0.1 (*Pe*=900).

At *Re*=0.2 (*Pe*=1800), the overall increase in mixing efficiency is 27% when block height is varied from

0.25 to 0.75. As the block height is varied from 0.25 to 0.75, the overall increase in mixing efficiency is 21.9% at *Re*=0.1 (*Pe*=900). Whereas the overall increase in mixing efficiency is 18.3 % when block height is varied from 0.25 to 0.75 at *Re*=0.05 (*Pe*=450). In short, increasing the block height for a fixed *Re* and *Pe* will enhance the mixing efficiency. As the height of the rectangular block decreased from 0.75 to 0.25, mixing due to convection gradually decayed. Due to more surface contacts between mixing fluids, concentration gradient across the mixing micro-channel is elevated in the constricted region which leads to high diffusive flux. Also, the width of inter diffusion zone is high, which provide more possibilities to fluid molecules for diffuse across each other and enhance the mixing process.

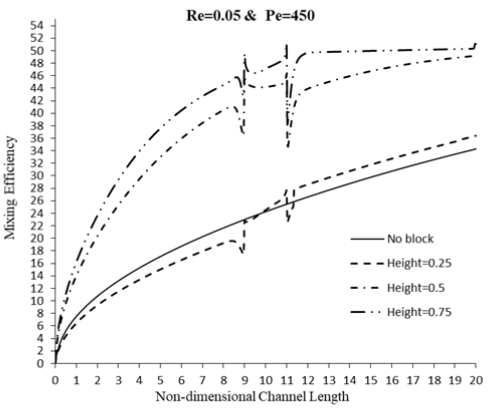

Fig. 20. Enhancement of species mixing efficiency obtained by varying the block height at *Re*=0.05 (*Pe*=450).

Table 2 Mixing efficiency at micro-channel outlet for varied heights of rectangular block at different *Re* and *Pe*.

Re	*Pe*	Non-dimensional height of rectangular block		
		0.25	0.5	0.75
0.2	1800	23	44	50
0.1	900	29	47	50.9
0.05	450	33	49	51.3

In general, the results show that the flow perturbations introduced by rectangular block of various heights improve the mixing performance compared to that achieved in a straight micro-channel. Increasing the height not only increases the interfacial contact area between the two species, but also extends the retention time. Therefore, the mixing efficiency is improved, particularly for rectangular block of maximum height.

4. CONCLUSION

In the smooth and straight mixing channel, mixing is purely diffusive in nature and therefore, the mixing efficiency is very low and demands more length for the channel. The numerical analysis indicates that the introduction of rectangular block varied in height along with electro-osmotic effects within the mixing channel enhances the mixing efficiency significantly by forcing the bulk flow to pass through the constricted regions above the rectangular block.

4.1. Major Remarks

- A modified IBM is used for numerical simulation of pressure driven electro-osmotic flow and mixing in a constricted (rectangular block of varied heights) micro-channel on staggered grid with finite-volume discretization of the following governing equations (i) Poisson-Boltzmann equation, (ii) Continuity equation, (iii) Momentum equation, and (iv) Species concentration equation.
- The numerical code is developed using Digital Visual FORTRAN (DVF)
- This research work incorporates both active and passive mixing techniques together to enhance the mixing efficiency in micro-channel as it considers electro-osmotic effects and channel constriction simultaneously. Hence it may be considered as a hybrid technique.
- The effects of various parameters like heights of the rectangular block, Reynolds number (Re), Peclet number (Pe), wall or zeta potential, external electric field and electrical double layer (EDL) thickness on mixing efficiency are studied. The maximum efficiency in this micro mixer design is found to be 51.3% for Reynolds number of 0.05 and Peclet number of 450 with the rectangular block height of 0.75.

The major advantages associated with the proposed modified IBM include easy grid generation, computer memory and CPU time savings. The significant disadvantages associated with the use of electro-osmotic flow are (i) high applied potentials are required to generate significant flow velocities, (ii) compatible only with a limited class of fluids (specifically low ionic concentration, aqueous solutions etc), and (iii) extreme sensitivity to surface conditions.

The major limitations are that the fundamental mixing mechanisms of fluid stretching and fluid folding are not considered in the present numerical simulations.

APPENDIX

$$\nabla^2\psi = -\frac{4\pi\rho_e}{D} \tag{I}$$

Here $\rho_e = ze(C_p - C_m)$ and assuming Boltzman distribution of the ions near a charged surface.

Hence we have

$$C_p = C_0 \exp\left[-\frac{ze\psi}{k_b T}\right] \; and \; C_m = C_0 \exp\left[\frac{ze\psi}{k_b T}\right].$$

Therefore, the electric charge density ρ_e is given by:

$$\rho_e = -2zen_0 \sinh\left[\frac{ze\psi}{k_b T}\right] \tag{II}$$

Substituting Eq. (II) in Eq. (I), we have

$$\nabla^2\psi = \frac{8\pi zen_0}{D}\sinh\left[\frac{ze\zeta}{k_b T}\right] \tag{III}$$

Now on substituting $\frac{\rho_e}{\rho}E_i = -\frac{D}{4\pi\rho}E_i\nabla^2\psi$ in Eq. (1), we get

$$\frac{\partial u_i}{\partial t} + \frac{\partial}{\partial x_j}(u_i u_j) = -\frac{1}{\rho}\frac{\partial p}{\partial x_i} + \frac{\mu}{\rho}\frac{\partial^2 u_i}{\partial x_j \partial x_j} - \frac{DE_i}{4\pi\rho}\nabla^2\psi + f_i \tag{IV}$$

For the purpose of making parametric studies, the following non-dimensional parameters are introduced:

$$L_{ref} = H, t^* = \frac{tu_{ref}}{H}, \; x^* = \frac{x}{H},$$
$$y^* = \frac{y}{H}, \psi^* = \frac{\psi}{\zeta}, u^* = \frac{u}{u_{ref}},$$
$$v^* = \frac{u}{u_{ref}}, \; P^* = \frac{P}{\rho u_{ref}^2},$$
$$C^* = \frac{C}{C_0}, \mathrm{Re} = \frac{\rho u_{ref} H}{\mu}, \; Pe = \frac{u_{ref} H}{D_i}$$

Normalization of velocity is carried out by using the Helomholtz-Smoluchowski velocity $\left(-\frac{E_x \varepsilon\varepsilon_0 \zeta}{\mu}\right)$.

The variables with superscript (*) indicate non-dimensional forms of the respective variables. The non-dimensional governing equation (Poisson-Boltzmann equation) for electric potential becomes:

$$\nabla^2\psi^* = \frac{8\pi zen_0}{D}\sinh\left[\frac{ze\zeta}{k_b T}\right]\psi^* \tag{V}$$

Defining ionic energy parameter, $\alpha = \frac{ze\zeta}{k_b T}$, the non-dimensional parameter relating $\alpha, \omega \; and \; H$ is $\beta = \frac{(\omega \mathrm{H})^2}{\alpha}$, where in $\omega = \frac{1}{\lambda} = \sqrt{\frac{8\pi z^2 e^2 n_0}{Dk_b T}}$. Hence Eq. (V) becomes:

$$\nabla^2\psi^* = \beta \sinh\left[\alpha\psi^*\right] \tag{VI}$$

Substitute Eq. (VI) in Eq. (IV) with normalization, we get Eqs. (4), (5) and (6) to be solved numerically.

ACKNOWLEDGEMENTS

The authors extend their appreciation to the Deanship of Scientific Research at King Khalid University, Saudi Arabia for funding this work through research groups program under grant number (R.G.P.1/58/39).

REFERENCES

Ababaei, A., A. A. Arani and A. Aghaei (2017). Numerical investigation of forced convection of nanofluid flow in microchannels: effect of adding micromixer. *Journal of Applied Fluid Mechanics 10*, 1759-1772.

Ahmed, D., X. Mao, B. K. Juluri and T. J. Huang (2009). A fast microfluidic mixer based on acoustically driven sidewall-trapped microbubbles. *Microfluidics and nanofluidics 7*(5), 727.

Aubin, J., D. F. Fletcher and C. Xuereb (2005). Design of micromixers using CFD modelling. *Chemical Engineering Science 60*(8-9), 2503-2516.

Azis, M. H. A., F. Evrard and B. van Wachem (2019). An immersed boundary method for incompressible flows in complex domains. *Journal of Computational Physics 378*, 770-795.

Babaie, A., A. Sadeghi and M. H. Saidi (2011). Combined electroosmotically and pressure driven flow of power-law fluids in a slit microchannel. *Journal of Non-Newtonian Fluid Mechanics 166*(14-15), 792-798.

Banerjee, A., A. K. Nayak and B. Weigand. (2019). Enhanced mixing and flow reversal in a modulated microchannel. *International Journal of Mechanical Sciences* 155, 430-439.

Bera, S. and S. Bhattacharyya (2013). On mixed electroosmotic-pressure driven flow and mass transport in microchannels. *International Journal of Engineering Science 62*, 165-176.

Bhattacharyya, S. and S. Bera (2015). Combined electroosmosis-pressure driven flow and mixing in a microchannel with surface heterogeneity. *Applied Mathematical Modelling 39*(15), 4337-4350.

Baum, J., H. Luo and R. Loehner (1998). The numerical simulation of strongly unsteady flows with hundreds of moving bodies. In *36th AIAA Aerospace Sciences Meeting and Exhibit*, 788.

Bayraktar, T., and S. B. Pidugu (2006). Characterization of liquid flows in microfluidic systems. *International Journal of Heat and Mass Transfer 49*(5-6), 815-824.

Bianchi, F., R. Ferrigno and H. H. Girault (2000). Finite element simulation of an electroosmotic-driven flow division at a T-junction of microscale dimensions. *Analytical Chemistry 72*(9), 1987-1993.

Borgohain, P., A. Dalal, G. Natarajan and H. P. Gadgil (2018). Numerical assessment of mixing performances in cross-T microchannel with curved ribs. *Microsystem Technologies* 24(4), 1949-1963.

Buchegger, W., C. Wagner, B. Lendl, M. Kraft and M. J. Vellekoop (2011). A highly uniform lamination micromixer with wedge shaped inlet channels for time resolved infrared spectroscopy. *Microfluidics and Nanofluidics* 10(4), 889-897.

Burgreen, D. and F. R. Nakache (1964). Electrokinetic flow in ultrafine capillary slits1. *The Journal of Physical Chemistry* 68(5), 1084-1091.

Campisi, M., D. Accoto, F. Damiani and P. Dario (2009). A soft-lithographed chaotic electrokinetic micromixer for efficient chemical reactions in lab-on-chips. *Journal of Micro-Nano Mechatronics* 5(3-4), 69-76.

Chang, C. C. and R. J. Yang (2004). Computational analysis of electrokinetically driven flow mixing in microchannels with patterned blocks. *Journal of Micromechanics and Microengineering* 14(4), 550.

Chen, S., T. Zhang, L. Lv, Y. Chen, Y. Yang and S. Tang (2019). Intensification of the liquid side mass transfer in double-side falling film microchannels by micro-mixing structures. *Chemical Engineering Science* 193, 264-275.

Cho, C. C. (2007). Electrokinetically-driven flow mixing in microchannels with wavy surface. *Journal of colloid and interface science* 312(2), 470-480.

Cho, C. C. (2008). Electrokinetically driven flow mixing utilizing chaotic electric fields. *Microfluidics and nanofluidics* 5(6), 785-793.

Cummings, E. B., S. K. Griffiths and R. H. Nilson (1999, August). Irrotationality of uniform electro-osmosis. In *Microfluidic Devices and Systems II* 3877, 180-190. International Society for Optics and Photonics.

Du, Y., Z. Zhang, C. Yim, M. Lin and X. Cao (2010). A simplified design of the staggered herringbone micromixer for practical applications. *Biomicrofluidics* 4(2), 024105.

Dutta, P. and A. Beskok (2001). Analytical solution of combined electroosmotic/pressure driven flows in two-dimensional straight channels: finite Debye layer effects. *Analytical chemistry* 73(9), 1979-1986.

Dutta, P., M. J. Kim, K. D. Kihm and A. Beskok (2001, November). Electroosmotic flow in a grooved micro-channel configuration: a comparative study of μPIV measurements and numerical simulations. In *Proceedings of 2001 ASME international mechanical engineering congress and exposition, New York, NY, USA*, 11-16.

Dutta, P., A. Beskok and T. C. Warburton (2002a). Numerical simulation of mixed electroosmotic/pressure driven microflows. *Numerical Heat Transfer: Part A: Applications* 41(2), 131-148.

Dutta, P., A. Beskok and T. C. Warburton (2002b). Electroosmotic flow control in complex microgeometries. *Journal of Microelectromechanical Systems* 11(1), 36-44.

Ebrahimi, S., A. Hasanzadeh-Barforoushi, A. Nejat, and F. Kowsary (2014). Numerical study of mixing and heat transfer in mixed electroosmotic/pressure driven flow through T-shaped microchannels. *International Journal of Heat and Mass Transfer* 75, 565-580.

Fan, J., S. Li, Z. Wu and Z. Chen (2019). Diffusion and mixing in microfluidic devices. In *Microfluidics for Pharmaceutical Applications* (79-100). William Andrew Publishing.

Harlow, F. H. and J. E. Welch (1965). Numerical calculation of time- dependent viscous incompressible flow of fluid with free surface. *The physics of fluids* 8(12), 2182-2189.

Herr, A. E., J. I. Molho, J. G. Santiago, M. G. Mungal, T. W. Kenny and M. G. Garguilo (2000). Electroosmotic capillary flow with nonuniform zeta potential. *Analytical chemistry* 72(5), 1053-1057.

Isfahani, A. M., R. Nasehi and E. Shirani (2018). Mixing enhancement in microchannels using thermo-viscous expansion by oscillating temperature wave. *Chemical Engineering and Processing-Process Intensification 126*, 123-131.

Islami, S. B. and M. Khezerloo (2017). Enhancement of Mixing Performance of Non-Newtonian Fluids using Curving and Grooving of Microchannels. *Journal of Applied Fluid Mechanics* 10(1), 127-141.

Jens, J., D. Te and R. Zengerle (2010). *Microfluidics*. Springer Verlag, Edition 1, ISBN: 3540201882.

Keh, H. J. and Y. C. Liu (1995). Electrokinetic flow in a circular capillary with a surface charge layer. *Journal of colloid and interface science* 172(1), 222-229.

Kim, J., D. Kim and H. Choi (2001). An immersed-boundary finite-volume method for simulations of flow in complex geometries. *Journal of Computational Physics* 171(1), 132-150.

Kim, M., A. Beskok and K. Kihm (2002). Electro-osmosis-driven micro-channel flows: A comparative study of microscopic particle image velocimetry measurements and numerical simulations. *Experiments in Fluids* 33(1), 170-180.

Lim, C. Y., Y. C. Lam and C. Yang (2010). Mixing enhancement in microfluidic channel with a constriction under periodic electro-osmotic flow. *Biomicrofluidics 4*(1), 014101.

Lo, W. Y., and K. Y. Chan (1994). Poisson–

Boltzmann calculations of ions in charged capillaries. *The Journal of chemical physics* 101(2), 1431-1434.

Luong, T. D., V. N. Phan and N. T. Nguyen (2011). High-throughput micromixers based on acoustic streaming induced by surface acoustic wave. *Microfluidics and nanofluidics* 10(3), 619-625.

Mahammedi, A., H. Ameur and A. Ariss (2017). Numerical Investigation of the Performance of Kenics Static Mixers for the Agitation of Shear Thinning Fluids. *Journal of Applied Fluid Mechanics 10*(3), 989-999.

Mittal, R. and G. Iaccarino (2005). Immersed boundary methods. *Annual Review of Fluid Mechanics* 37, 239-261.

Molho, J. I., A. E. Herr, M. Desphande, J. R. Gilbert, M.G. Garguilo, P. H. Paul, ... & C. Connel (1998). Fluid transport mechanisms in microfluidic devices. *Proc. ASME Micro-Electro-Mechanical-Systems* (MEMS), 66, 69-76.

Mollajan, M., S. R. Bazaz and A. A. Mehrizi (2018). A Thoroughgoing Design of a Rapid-cycle Microfluidic Droplet-based PCR Device to Amplify Rare DNA Strands. *Journal of Applied Fluid Mechanics* 11(1), 21-29.

Nayak, A. K., A. Banerjee and B. Weigand (2018). Mixing and charge transfer in a nanofluidic system due to a patterned surface. *Applied Mathematical Modelling* 54, 483-501.

Neerincx, P. E., R. P. Denteneer, S. Peelen and H. E. Meijer (2011). Compact mixing using multiple splitting, stretching, and recombining flows. *Macromolecular Materials and Engineering* 296(3- 4), 349-361.

Ohshima, H. and T. Kondo (1990). Electrokinetic flow between two parallel plates with surface charge layers: electro-osmosis and streaming potential. *Journal of colloid and interface science* 135(2), 443-448.

Patankar, N. A., and H. H. Hu (1998). Numerical simulation of electroosmotic flow. *Analytical Chemistry* 70(9), 1870-1881.

Paul, P. H., M. G. Garguilo and D. J. Rakestraw (1998). Imaging of pressure-and electrokinetically driven flows through open capillaries. *Analytical Chemistry* 70(13), 2459-2467.

Peskin, C. S. (1972). Flow patterns around heart valves: a numerical method. *Journal of computational physics* 10(2), 252-271.

Probstein, R. F. (2005). *Physicochemical hydrodynamics: an introduction*. John Wiley & Sons.

Qaderi, A., J. Jafar and B. Mehdi (2019). CFD simulation of combined electroosmotic-pressure driven micro-mixing in a microchannel equipped with triangular hurdle and zeta-potential heterogeneity. *Chemical Engineering Science* 199, 463-477.

Ramamurti, R. and W. Sandberg (2001). Simulation of flow about flapping airfoils using finite element incompressible flow solver. *AIAA journal 39*(2), 253-260.

Ren, W., C. Shu and W. Yang (2013). An efficient immersed boundary method for thermal flow problems with heat flux boundary conditions. *International Journal of Heat and Mass Transfer 64*, 694-705.

Reuss, F. F. (1809). Sur un nouvel effet de l'électricité galvanique. *Mem. Soc. Imp. Natur. Moscou 2*, 327-337.

Rice, C. L. and R. Whitehead (1965). Electrokinetic flow in a narrow cylindrical capillary. *The Journal of Physical Chemistry* 69(11), 4017-4024.

Saleel, C. A., A. Shaija and S. Jayaraj (2011). Numerical simulation of fluid flow over a forward–backward facing step using immersed boundary method. *International Journal of Engineering Science and Technology* 3(10), 7714-7729

Saleel, C. A., A. Shaija and S. Jayaraj (2013). Computational simulation of fluid flow over a triangular step using immersed boundary method. *International Journal of Computational Methods* 10(4), 1350016.

Santiago, J. G. (2001). Electroosmotic flows in microchannels with finite inertial and pressure forces. *Analytical chemistry* 73(10), 2353-2365.

Tezduyar, T. E. (2001). Finite element methods for flow problems with moving boundaries and interfaces. Archives of Computational Methods in Engineering 8(2), 83.

Wang, Z., J. Fan, K. Luo and K. Cen (2009). Immersed boundary method for the simulation of flows with heat transfer. *International Journal of Heat and Mass Transfer* 52(19-20), 4510-4518.

Wang, D., J. Summers and P. H. Gaskell (2007). Modeling of electrokinetically driven flow mixing enhancement in microchannels with patterned heterogeneous surface and blocks. *Nanoscale and microscale thermophysical engineering* 11(1-2), 1-13.

Yang, R. J., L. M. Fu and Y. C. Lin (2001). Electroosmotic flow in microchannels. *Journal of colloid and interface science* 239(1), 98-105.

Yang, C., and D. Li (1998). Analysis of electrokinetic effects on the liquid flow in rectangular microchannels. *Colloids and surfaces A: physicochemical and engineering aspects* 143(2-3), 339-353.